Photoreductive elimination of PhCl across the dinuclear core of a [GePt]^{VI} complex

Mohammadjavad Karimi and François P. Gabbaï*

Department of Chemistry, Texas A&M University, College Station, TX 77843, USA

ABSTRACT: As part of our interest in the photochemistry of platinum/p-block element complexes, we now report on the synthesis and photoreduction of $[(Ph)((o-Ph_2P)C_6H_4)_2GePtCl_3]$ (2-Ph), a complex featuring a tetravalent platinum center connected to a germyl ligand. When in the presence of a chlorine trap, 2-Ph undergoes a clean photolysis that affords $[(Ph)((o-Ph_2P)C_6H_4)_2GePtCl]$ (1-Ph) and $[(Cl)((o-Ph_2P)C_6H_4)_2GePtCl]$ (1-Cl) as confirmed by NMR spectroscopy. While the formation of 1-Ph results from the elimination of a chlorine equivalent from 2-Ph, the formation of 1-Cl indicates chlorobenzene elimination, which was confirmed and quantified using GC-MS. These results provide a unique example of a germanium-centered light-induced reduction process resulting in the *ipso*-chlorination of a phenyl-germanium species.

Introduction

In recent years, the HX (X=halogen) splitting reaction has been heavily investigated as a viable pathway towards solar energy conversion and storage.1 When mediated by transition metals, the HX splitting reaction involves an unfavorable energetically halogen photoreductive elimination step that limits the efficiency of the splitting process.1a, 1c To better understand the factors that govern this chemistry and identify platforms that support the facile light-induced elimination of halogens, high valent transition metal complexes based on PtIV, NiIII, and AuIII have been investigated.2 More recently, this field has witnessed the advent of high-valent main group complexes such as the Te^{IV} system **A** and the Sb^V system **B** (Figure 1)³ Additionally, with the view that dinuclear transition metal complexes with multiple available oxidation states could better accommodate the reaction intermediates involved in X• dissociation,1a a number of dinuclear transition metal complexes featuring PtIII-PtIII, PtIII-RhII, RhI-RhIII, IrII-AuII, and Pt^{III}-Au^{II} cores⁴ have been synthesized and demonstrated to undergo photoreductive elimination of Cl₂ equivalents. This strategy has also been extended to hybrid transition metal/main group complexes,⁵ such as **C** which eliminates a chlorine equivalent across the dinuclear Pd^{II}-Sb^V core.⁶ A similar observation was made in the case of the PtII-GeIV system **D** which can be photoreduced into 1-Cl, presumably through the intermediacy of **2**-Cl (Figure 1).⁷ To better understand the role played by the germanium substituents in these complexes, we have now decided to synthesize and investigate the properties 2-Ph, an analog of 2-Cl in which the germanium-bound chlorine atom is replaced by a phenyl group.

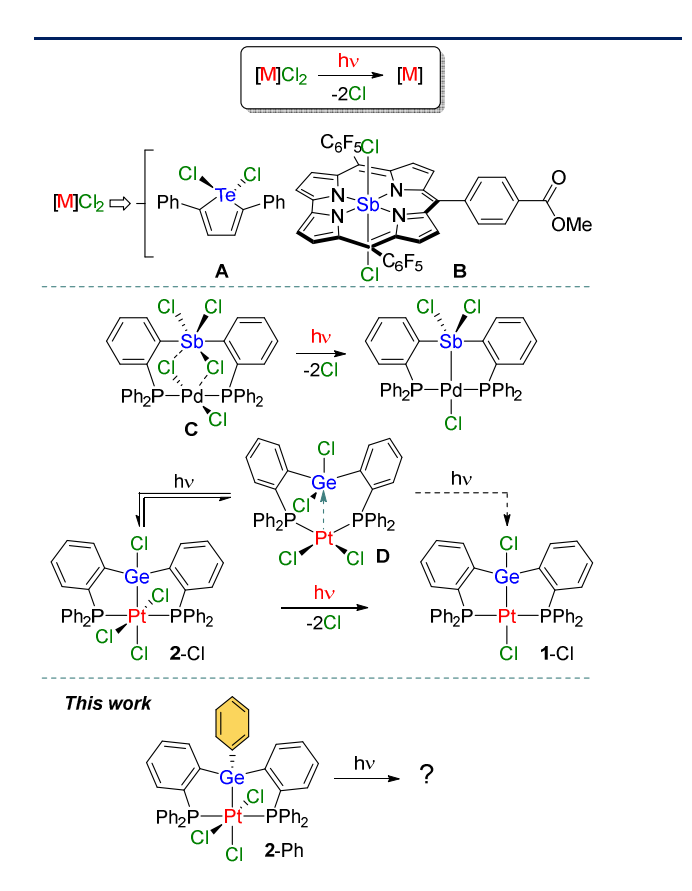


Figure 1. Examples of photoreductive elimination of chlorine supported by main group elements, and the objective of the current study.

Results and discussion

As an entry point, we targeted complex **1**-Ph. (Figure 1). Reaction of the known ligand (Ph)(Cl)(o-dppp)₂Ge (o-dppp = o-(Ph₂P)C₆H₄)⁸ with [(Ph₃P)₂Pt(C₂H₄)] proceeds with oxidative addition of the Ge–Cl bond on Pt, affording complex **1**-Ph (Scheme 1). This complex, which is reminiscent

of the known palladium catalysts of general formula [(o- $(R_2P)C_6H_4)_2$ GeMe]PdCl (R = alkyl or aryl group), gives rise to a single peak at 56.2 ppm in the ³¹P NMR spectrum, flanked by ¹⁹⁵Pt satellites. The ³¹P NMR chemical shift and the ¹/_{Pt-P} coupling constant of 3003 Hz are comparable to that of [(o-dppp)₂GeCl]PtCl (2-Cl),⁷ which shows a single peak at 57.8 ppm (${}^{1}J_{Pt-P}$ = 2885 Hz), as well as the PGeP pincer complex [PtCl{ $\kappa^3 P$,Ge,P-GeCl(NCH₂P t Bu₂)₂C₆H₄}c) (E, Figure 2) (${}^{1}J_{Pt-P}$ = 2836.0 Hz). 10 This bench-stable complex was also characterized by X-ray crystallography. Because of the constraints imposed by the pincer ligand, the divalent platinum adopts a distorted square planar coordination geometry characterized by a notable departure of the P-Pt-P angle (165.41(2)°) from linearity (Figure 3a). The same geometrical constraints affect the tetrahedral coordination geometry of the germanium atom as indicated by the larger than expected C6-Ge-C20 angle of 118.08(7)°. The Pt-Ge and Pt-Cl bond distances of 2.3572(5) Å and 2.3915(7) Å are similar to those of the previously reported complex **1**-Cl (2.3338(4) Å and 2.3891(8) Å respectively),⁷ as well as the PGeP pincer complexes E and F (Figure 2) reported by Cabeza (Pt-Ge distances 2.3017(5) Å and 2.3140(8) Å), $^{10-11}$ as well as that seen in [ClPtGe(o-dppp)₃] (**G**, Figure 2) described by Braun (Ge-Pt distance: 2.3545(2) Å).12

Scheme 1. Synthesis of complexes 1-Ph and 2-Ph.

Figure 2. Pt/Ge complexes of relevance to this study.

Oxidation of **1**-Ph with one equivalent of PhICl₂ in CH_2Cl_2 affords the target complex **2**-Ph quantitatively. This compound is characterized by a single resonance in the ³¹P NMR spectrum at 33.5 ppm with ¹⁹⁵Pt satellites (${}^1J_{Pt-P} = 1888 \text{ Hz}$), pointing to a formal oxidation state of +4 at the Pt center. Crystals suitable for X-ray analysis were readily obtained by diffusion of Et₂O into a CHCl₃ solution of **2**-Ph, and its structure is displayed in Figure 3b. The tetravalent platinum adopts an octahedral coordination geometry with Cl1-Pt-Cl3 (176.32(6°) and Ge-Pt-Cl2 (176.32(4)°) angles close to linearity. However, as in **1**-Ph, a notable departure from the ideal value of 180° is observed for the P-Pt-P angle (166.60(6)°). The tetrahedral coordination geometry

of the germanium atom in **2**-Ph also remains distorted as indicated by the large C6-Ge-C20 angle of 117.6(3)°. The Pt-Ge bond length of 2.4135(8) Å in this complex is slightly longer than that in **2**-Cl (2.3892(6) Å), and the Pt-Cl1 and Pt-Cl3 bond lengths of 2.3213(17) Å and 2.3353(16) Å are similar to the corresponding distances in **2**-Cl (2.3472(11) Å and 2.3075(11) Å, respectively.⁷ The stronger trans influence of the germyl moiety, however, results in the Pt-Cl2 linkage (2.4718(16) Å) being longer than the other Pt-Cl bonds, similar to the effect observed in its analog **2**-Cl.⁷

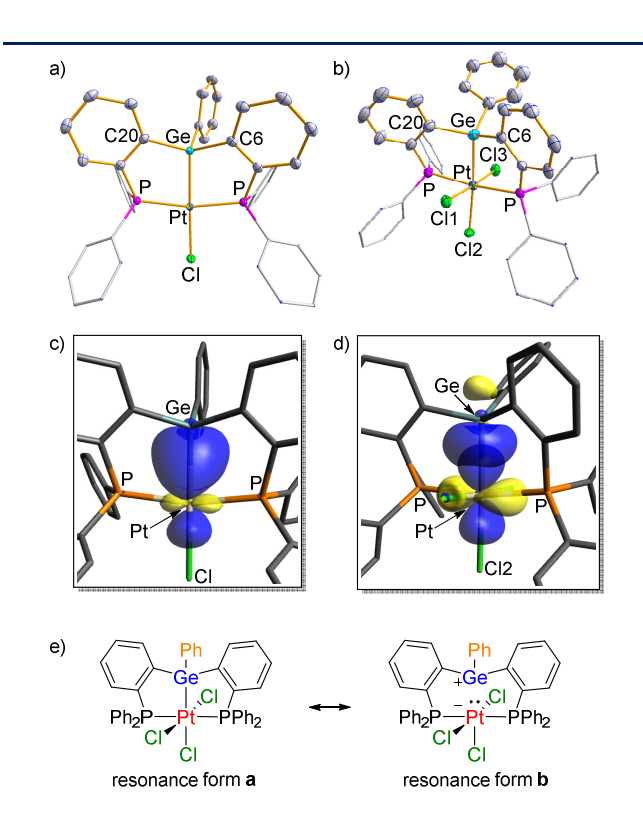


Figure 3. Solid-state structures of **1**-Ph (a) and **2**-Ph (b). Ellipsoids are drawn at the 50% probability level. H atoms and lattice solvent molecules are omitted for clarity, and the phenyl groups on the phosphines are drawn in wireframe. (c) NBO plot of the Pt-Ge bond in **1**-Ph, plotted at an isovalue of 0.05. (d) NBO plot of the Pt-Ge donor-acceptor interaction in **2**-Ph, plotted at an isovalue of 0.05. $E^2 = 58.52$ kcal mol⁻¹. (e) Relevant resonance forms of **2**-Ph.

Analysis of the electronic structure of **1**-Ph by NBO shows that the Pt–Ge σ -bond is mainly covalent (Figure 3c). In fact, an NLMO analysis indicates that contributions from Ge (46.02%) and Pt (53.98%) are close to one another, further supporting the covalent nature of this bond. A different bonding picture arises for **2**-Ph, where the Pt–Ge σ -bond is described as a dative bond involving donation of a lone pair from a d orbital on platinum to the empty p orbital on germanium (Figure 3d). Such interactions are well-known in the adducts of Lewis basic platinum complexes with Lewis acidic main group elements, such as [(Cy₃P)₂Pt \rightarrow GeCl₂] (**H**, Figure 2).¹³ The Ge-Pt bonding in **2**-Ph can be best explained by involving two resonance forms including one in which the divalent anionic platinate donates two electrons to the Lewis acidic germylium cation

(Figure 3e). In agreement with this description, the second-order perturbation energy of the Pt \rightarrow Ge interaction in **2**-Ph E^2 = 58.52 kcal mol⁻¹ is much lower than the E^2 = 83.11 kcal mol⁻¹ reported for **2**-Cl at the same level of theory,⁷ consistent with the lower Lewis acidity of a phenylgermylium versus that of a chlorogermylium.

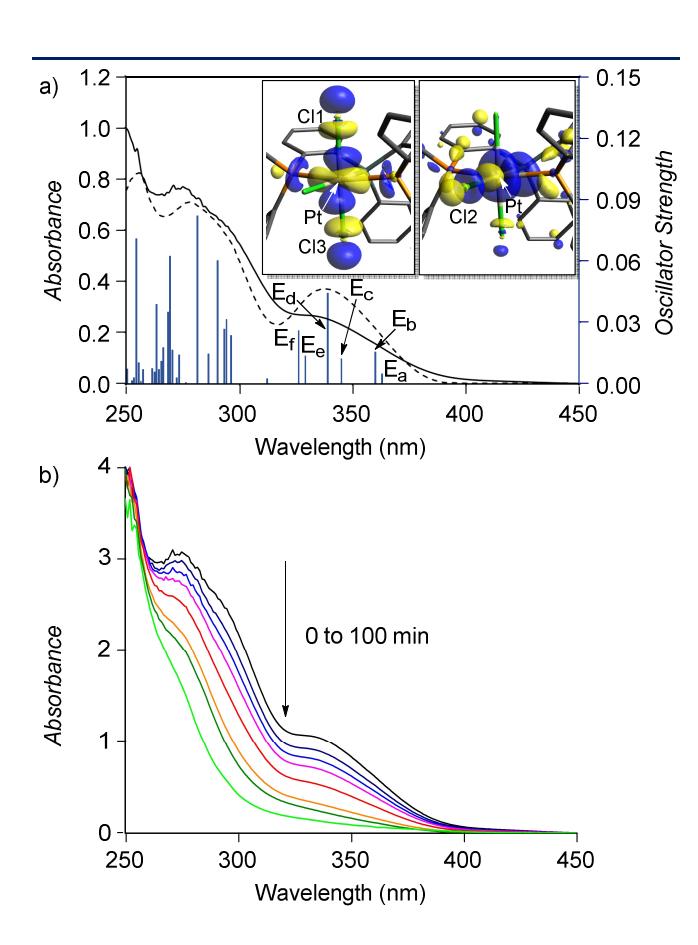


Figure 4. a) Experimental (solid) and predicted (dashed) UV–Vis spectra of **2**-Ph. Calculated vertical electronic transitions are represented by blue bars. The inset shows the calculated LUMO (left) and LUMO+1 (right) plotted at an isovalue of 0.05. b) UV-Vis monitoring of the photolysis of **2**-Ph (5.0 × 10^{-4} M) irradiated at 334 nm in the presence of 50 equivalents of SMe₂ in CH₂Cl₂. The black, navy, blue, purple, red, orange, dark green, and light green traces correspond to t=0, 10, 20, 33, 46, 60, 75, and 100 minutes respectively. A 75 W Xenon arc lamp was used for this experiment.

This compound displays absorption maxima at 270 and 334 nm in the UV-Vis spectrum (Figure 4a), with the bands blue-shifted by 30 and 16 nm with respect to those of 2-Cl. The origins of these bands were investigated by Time-Dependent Density Functional Theory (TD-DFT) at the MPW1PW91 level of theory (Gaussian 16 program, basis sets Pt, cc-pVTZ-PP; Ge, cc-pVTZ; P/Cl, 6-311+g(d,p); C/H 6-31g). The lower energy feature at 334 nm is described as an LMCT band arising from charge transfer from orbitals with large Cl1 and Cl3 lone pair character (Figure 4a, E_a - E_b , inset, Figure S11) to the Pt-Cl antibonding orbitals (LUMO and LUMO+1, Figure 4a inset, Figure S11), while the higher energy feature at 270 nm results from charge

transfer from orbitals with large Cl2 lone pair character to Pt–Cl antibonding orbitals. These assignments are in line with previous reports on Pt(IV) chloride complexes that undergo photoreductive chlorine evolution,⁵ and support the possibility of Cl[•] dissociation upon irradiation, eventually leading to formation of the photoproducts.

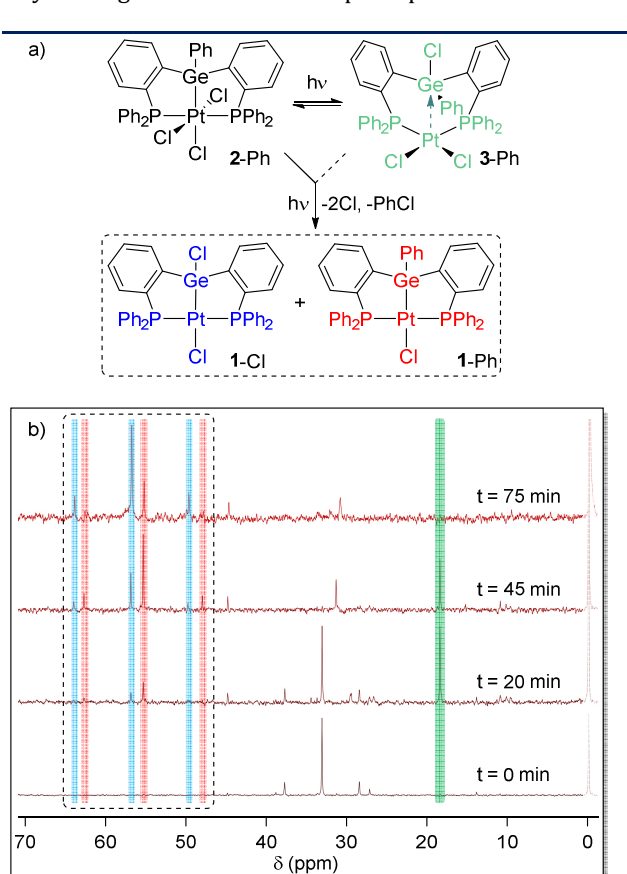


Figure 5. a) Reaction scheme for the photolysis of **2**-Ph. b) Photolysis of a 0.020 M solution of **2**-Ph in CH_2Cl_2 in the presence of 50 equivalents of SMe_2 monitored by ^{31}P NMR. A 100 W mercury arc lamp with no filter was used for this study. A sealed capillary containing H_3PO_4 was used as an internal standard, and its peak is faded in the spectra. The peaks corresponding to **1**-Ph, **1**-Cl, and **3**-Ph are marked by red, blue, and green respectively.

Encouraged by these results, we decided to study the photolysis of 2-Ph in CH₂Cl₂. Irradiation of solutions of 2-Ph in CH₂Cl₂ however, resulted in the formation of an amorphous brown material, suggesting decomposition of the complex. Addition of SMe2 as a chlorine trap to prevent oxidative damage to the complex resulted in a clean reaction. When a 5.0×10^{-4} M solution of 2-Ph was irradiated at 334 nm in the presence of 50 equivalents of SMe₂ using the monochromated light of a xenon lamp inside a fluorimeter, progressive quenching of the absorption bands was observed (Figure 4b). Time-dependent analysis of the absorption quenching with respect to ferrioxalate as a standard actinometer yields a photochemical quantum yield of 2.7%, which is in agreement with those obtained for tetravalent platinum complexes supported by main group ligands,5 and closely resembles that of 2-Cl (3.2%).7 When this photoreaction is monitored by ³¹P NMR spectroscopy, we observed that, in the first few minutes of photolysis, consumption of **2**-Ph marked by a gradual decrease of the intensity of the peak at 33.5 ppm, is accompanied by two peaks corresponding to **1**-Ph at 56.2 ppm and **1**-Cl at 57.8 ppm (Figure 5b). Integration of all the peaks with respect to H_3PO_4 in a sealed capillary as an internal standard shows negligible loss of material, as well as a 56:44 ratio of **1**-Cl to **1**-Ph.

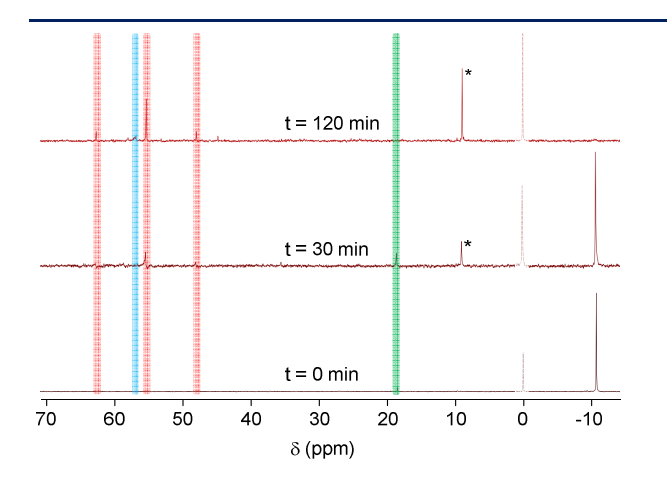


Figure 6. ^{31}P NMR spectra of a solution of the ligand (Ph)(Cl)(o-dppp) $_2$ Ge (2.8 mM) and PtCl $_2$ (SMe $_2$) $_2$ (2.8 mM) in CH $_2$ Cl $_2$ in the presence of 50 equivalents of SMe $_2$, irradiated using a 100 W mercury arc lamp. A sealed capillary containing H $_3$ PO $_4$ was used as an internal standard and its peak is faded in the spectra. The peaks corresponding to **1**-Ph, **1**-Cl, and **3**-Ph are marked by red, blue, and green, respectively. Formation of the oxidized ligand is marked by an asterisk in the spectra. The same peak was observed when the ligand (Ph)(Cl)(o-dppp) $_2$ Ge was treated with 2 equivalents of PhICl $_2$ in CH $_2$ Cl $_2$.

We also note the intermediate appearance of a peak at 18.6 ppm. We assign this resonance to 3-Ph (Figure 5a) on the basis of the similarity of its chemical shift and Pt-P coupling constant (${}^{1}/_{Pt-P} = 1730 \text{ Hz}$) to those reported for **D**.⁷ Independent attempts to synthesize this compound from the ligand (Ph)(Cl)(o-dppp)₂Ge and PtCl₂(SMe₂)₂ gave rise to the signal corresponding to this complex at 18.6 ppm. The formation of 3-Ph was incomplete when the ligand and Pt(II) reagents were mixed in equimolar amounts. Higher concentrations of the Pt(II) reagent led to increased but still incomplete formation of 3-Ph, indicating the existence of an equilibrium. Despite repeated efforts, 3-Ph could not be isolated. We assign the incomplete formation of this complex to the steric congestion introduced by the phenyl group on germanium. Interestingly, when the mixture containing (Ph)(Cl)(o-dppp)₂Ge and PtCl₂(SMe₂)₂ was irradiated in the presence of 50 equivalents of SMe2, both 1-Cl and 1-Ph were observed by 31P-NMR spectroscopy (Figure 6), suggesting that **3**-Ph is indeed a relevant species in the photolysis of 2-Ph. Irradiation of the free ligand for 1 hour in the presence of SMe2 did not result in any changes in the ³¹P NMR spectrum.

The intriguing loss of the phenyl group on the germanium atom upon irradiation suggests the possible formation of benzene or chlorobenzene as the byproducts of the photoreaction. When the final solution obtained after photolysis of a 0.020 M solution of 2-Ph in the presence of 50 equivalents of SMe2 was subjected to GC-MS analysis, chlorobenzene was the only relevant byproduct identified, ruling out benzene formation (Figure S8). This is further confirmed by direct observation of chlorobenzene by ¹³C NMR spectroscopy carried out on the same solution (Figure S7). Ouantitative analysis of this solution by GC-MS, against CH2Cl2 solutions of chlorobenzene with known concentrations afforded a chlorobenzene concentration of 9.6×10^{-3} M (Figure S9). This value is in good agreement with the relative concentration of 1-Cl obtained from the ratio of peak integrations in the 31P NMR spectrum at the end of photolysis (1.1 \times 10⁻² M), and further confirms that within the error limit of the measurements, all the phenyl groups abstracted from the ligand during the photolysis are converted to chlorobenzene.

Figure 7. Selected examples of relevant complexes that undergo reductive elimination of aryl chlorides.

Although oxidative addition of aryl chlorides on transition metal centers has been heavily investigated within the context of cross-coupling chemistry,14 the reverse of this fundamental reaction, namely the reductive elimination of arvl chlorides is of little precedence. Notable examples are reductive elimination of chlorobenzene from Ph₂SbCl₃ upon treatment with 2,2'-bipyridine and TMSOTf (Figure 7, I) reported by Burford et al.15, and photoreductive elimination of C₆F₅Cl from a Au(III)-carbene complex bearing two chlorides and a pentafluorophenyl ligand (Figure 7, II) reported by Rosenthal et al. 16,17 The latter example is especially interesting in that contrary to our system, as well as other precedent examples of gold(III) chloride complexes, it does not demonstrate Cl2 evolution at all but instead undergoes photoelimination of C₆F₅Cl, although this photoproduct was not quantified. Related aryl-chloride eliminations have also been observed upon thermolysis of arylated phosphine gold(III) chloride complexes18 such as Ph₃PAuCl(CF₃)(p-FC₆H₄) (Figure 7, III).¹⁹ While Rosenthal et al proposed a two electron pathway starting with dissociation of chloride, followed by its nucleophilic attack on the C₆F₅ ligand, a concerted pathway has been invoked in the case of the phosphine-based systems. 18-19 In the case of **2**-Ph, we believe that the first step of the process is dissociation of Cl*, which is supported by our TD-DFT studies (vide supra) as well as the detection of a Cl*-charge transfer complex in the photolysis of 2-Cl.^{2a, 4a, 7, 20} In the case of 2-Ph, we propose that the nascent Cl* undergoes quenching, either by SMe₂ or by the phenyl group on germanium to afford chlorobenzene. In support of this mechanistic proposal, when a 0.02 M solution of 2-Ph in CH₂Cl₂ was subjected to photolysis in the presence of 200 equivalents of SMe₂ instead of 50, phenyl abstraction was completely suppressed, and clean conversion to 1-Ph was observed (Figure S10). This can be interpreted as much more rapid quenching of the nascent Cl• when a large excess of SMe2 is present, therefore preventing it from attacking the germanium-bound phenyl group. The formation of chlorobenzene in this chemistry provides an example of an ipsohalogenation of a phenyl-germanium species. While such reactions are well documented and have been the subject of recent efforts,7 we are not aware of any precedents in which the reaction can be elicited by irradiation.

Conclusion

In summary, we describe the bifurcated photochemical reactivity of a novel high-valent PtGe complex (2-Ph) which eliminates either two chlorine atoms or an equivalent of chlorobenzene when irradiated with UV light. The formation of chlorobenzene was inferred based on the nature of the PtGe photoproduct (1-Cl) and confirmed by quantitative GC-MS analysis. These results show that the hybrid transition metal-main group complex 2-Ph, originally designed to photoeliminate chlorine, also supports the light-induced ipso-chlorination of the phenyl group bound to the germanium atom. This reactivity shows that the impetuous characteristic of the chlorine atom can be corralled to achieve a concerted C-Cl bond formation within the confine of the dinuclear PtGe core. Another noteworthy facet of this work is the unambiguous demonstration that the substituent attached to the main group element, in this case a phenyl group, participates in the photoreductive process.

Experimental Section

General considerations

Ethylenebis(triphenylphosphine)platinum(0) purchased from ACROS Organics and used as received. The ligand (o-(Ph₂P)C₆H₄)₂(Ph)GeCl,²¹ and PhICl₂²² were prepared as described in the literature. Air and moisture sensitive manipulations were carried out under an atmosphere of dry N2 using either a glove box or standard Schlenk techniques. Et₂O, THF, and toluene were dried by distillation over Na/K under N2. All other solvents were used as received. NMR spectra were recorded on a Varian Unity Inova 500 FT NMR spectrometer (499.42 MHz for ¹H, 125.58 MHz for ¹³C, 202.18 MHz for ³¹P). Chemical shifts (δ) are given in ppm and are referenced against residual solvent signals (1H, 13C) or external or internal H₃PO₄ (31P). Elemental analyses were performed at Atlantic Microlab (Norcross, GA). UV-vis. spectra were recorded on a Hewlett-Packard 8453 spectrophotometer equipped with a

dual tungsten/deuterium lamp source. A 75 W xenon lamp integrated in a PTI QuantaMaster 40 fluorescence spectrophotometer was used for monochromatic irradiations. A 100 W mercury arc lamp was used for the other experiments. GC-MS analysis was carried out using a HP 6890 Series chromatograph coupled with a HP 5973 mass analyzer. The GC was equipped with a J&W-122-5536 capillary column (length: 30 m, id: 0.250 mm, film thickness: $50 \mu m$), and helium was used as the carrier gas.

Synthesis of 1-Ph

The ligand $(Ph)(Cl)(o-(Ph_2P)C_6H_4)_2Ge$ (189 mg, 0.267 mmol) was added to solution ethylenebis(triphenylphosphine)platinum(0) (200 mg, 0.267 mmol) in THF (10 ml), and the mixture was stirred The solvent was removed under reduced pressure, and the crude mixture was washed with pentane (5x5mL) and dried under vacuum to afford **1**-Ph as a pale yellow powder. Yield: 200 mg (82.8%). Single crystals suitable for X-ray measurement were obtained by slow diffusion of hexanes into a solution of 1-Ph in toluene. ¹H NMR (499.42 MHz; CDCl₃): δ 8.12 (d, 2H, o-(Ge)C₆H₄, ³J_{H-H} = 7.3 Hz), 7.69 (m, 4H), 7.55 (m, 4H), 7.50 (t, 2H, ${}^{3}J_{H-H}$ =12.9 Hz), 7.39 (m, 8H), 7.32 (m, 8H), 6.90 (t, 1H, ${}^{3}J_{H-H}=14.8$ Hz, $(p-C_6H_5)Ge)$, 6.73 (t, 2H, ${}^3J_{H-H}=14.8$ Hz, $(m-C_6H_5)Ge)$, 6.56 (d, 2H, ${}^{3}I_{H-H}$ =7.8 Hz, (o-C₆H₅)Ge) ${}^{13}C$ { ${}^{1}H$ } NMR (125.66 MHz; CDCl₃): 151.8 (t, ${}^{1}J_{C-P}$ = 24.4 Hz, ipso C₆H₄Ge), 142.2 (t, $I_{C-P} = 14.1 \text{ Hz}$, ipso C_6H_5P), 134.1 (dt, $I_{C-P} = 6.3 \text{ Hz}$, $I_{C-P} = 2.8 \text{ Hz}$ Hz), 133.7 (s), 133.5 (t, J_{C-P} = 2.8 Hz), 133.4 (s),131,6 (dt, J_{C-P} P = 25.5 Hz, $I_{C-P} = 6.0 \text{ Hz}$, 130.8 (s), 130.6 (d, $I_{C-P} = 7.2 \text{ Hz}$), 129.4 (t, $J_{C-P} = 4.0 \text{ Hz}$), 128.7 (t, $J_{C-P} = 5.3 \text{ Hz}$), 128.3 (t, $J_{C-P} =$ 5.3 Hz), 127.6 (s) 127.3 (s). ³¹P {¹H} NMR (202.16 MHz; CDCl₃): 56.2 (s, ${}^{1}J_{Pt-P}$ = 3003 Hz). Elemental analysis for C₄₂H₃₃ClP₂GePt: Calculated (%) C, 55.88; H, 3.68; Found: C, 55.60; H, 3.55.

Synthesis of 2-Ph

PhICl₂ (14.6 mg, 0.0531 mmol) was added to a solution of $[(Ph)(o-(Ph_2P)C_6H_4)_2)GePtCl]$ (48.0 mg, 0.0531 mmol) in CH₂Cl₂ (2 ml), and the mixture was stirred for 20 minutes. The solvent was removed under vacuum, and the crude residue was washed with Et₂O (3x3mL) to afford 2-Ph as a yellow powder. Yield: 50.0 mg (96.6%). Single crystals suitable for X-ray analysis were obtained by diffusion of Et₂O into a CDCl₃ solution of **2-**Ph. ¹H NMR (499.42 MHz; CDCl₃): δ 8.12 (d, 2H, o-(Ge)C₆H₄, ${}^{3}J_{H-H}$ = 7.0 Hz), 8.06 (m, 4H), 7.62 (t, 2H, ${}^{3}J_{H-H}$ = 7.0 Hz), 7.58-7.51 (m, 8H), 7.47 (d, 2H, ${}^{3}J_{H-H}$ =6.8 Hz), 7.41 (t, 4H, ${}^{3}J_{H-H}$ =7.2 Hz), 7.30 (m, 6H), 7.07 (t, 1H, ${}^{3}J_{H-H}$ =7.1 Hz, (p-C₆H₅)Ge), 6.89 (t, 2H, ${}^{3}J_{H-H}$ =7.1 Hz, $(m-C_6H_5)Ge$), 6.77 (d, 2H, $^3I_{H-H}=7.1$ Hz, $(o-C_6H_5)Ge$). ^{13}C {1H} NMR (125.66 MHz; CDCl₃): δ 149.6 (t, ${}^{1}J_{C-P}$ = 19.6 Hz, ipso C_6H_4P), 136.6 (t, $J_{C-P}=5.3$ Hz), 135.4 (t, $J_{C-P}=3.5$ Hz), 134.9 (s), 134.6 (t, $J_{C-P} = 5.1 \text{ Hz}$), 131.7 (s), 131.3 (s), 129.6 $(t, I_{C-P} = 3.5 \text{ Hz}), 129.2 \text{ (s)}, 128.0 \text{ (t, } I_{C-P} = 5.3 \text{ Hz}), 127.6 \text{ (t, } I_{C-P} = 5.3 \text{ Hz})$ $_{P}$ = 5.4 Hz), 127.4 (s), 126.8, 126.1 (t, $^{1}J_{C-P}$ = 30.3 Hz, ipso C_6H_5P). ³¹P {¹H} NMR (202.16 MHz; CDCl₃): δ 33.5 (s, ¹ J_{Pt-P} = 1888 Hz). Elemental analysis calculated (%) for C₄₂H₃₃Cl₃P₂GePt: C, 51.81; H, 3.42; found: C, 51.48; H, 3.42 (average of two measurements).

Crystallographic Details

X-ray crystallographic datasets were collected at T = 110 K on a BRUKER Quest diffractometer (Mo source, λ = 0.71073 Å) equipped with a PHOTON III detector. Semi-empirical absorption corrections were implemented using the BRUKER SADABS program. 23 The structures were solved using the direct method by SHELXT 24 and the data was refined against F^2 by least squares cycles using SHELXL. 25 All non-H atoms were refined anisotropically. H atoms were refined using the riding atom model. CCDC 2101954-2101955 contain the supplementary crystallographic data for this paper.

Computational Details

All computations were carried out with the Gaussian 16 program²⁶ using the functional MPW1PW91 and the mixed basis set cc-pVTZ-PP for Pt, cc-pVTZ for Ge, 6-311+g(d,p) for P/Cl, 6-31g for C/H. Frequency calculations carried out on the optimized structures of the compounds confirmed the absence of any imaginary frequencies. NBO and NLMO analyses were carried out using the NBO 6.0 program.²⁷

Photolysis reactions monitored by ³¹P NMR spectroscopy

Photolysis of **2**-Ph: an NMR tube was charged with **2**-Ph (9.7 mg, 0.01 mmol), CH_2Cl_2 (0.5 mL), and SMe_2 (37 μ L, 0.5 mmol for 50 equivalents, or 148 μ L, 2.0 mmol for 200 equivalents) and a sealed capillary containing H_3PO_4 , and irradiated using a 100 W mercury arc lamp. ³¹P NMR spectra were recorded periodically over 90 minutes. No change was observed after 60 minutes.

Photolysis of **3**-Ph: an NMR tube was charged with the ligand (Ph)(Cl)(o-dppp)₂Ge (10.0 mg, 0.014 mmol) and PtCl₂(SMe₂)₂ (5.5 mg, 0.014 mmol). CH₂Cl₂ (0.45 mL) and SMe₂ (53 μ L, 70.6 mmol, 50 equivalents) were subsequently added along with a sealed capillary containing H₃PO₄. The solution was irradiated using a 100 W mercury arc lamp and ³¹P NMR spectra were recorded periodically over 2 hours. Figure 6 shows the reaction progress and formation of **1**-Ph and **1**-Cl. An extra peak at 9.0 ppm grows over time, presumably due to oxidation or decomposition of the free ligand. Similar results were observed by ³¹P NMR when solutions obtained upon stirring the ligand (Ph)(Cl)(o-dppp)₂Ge and PtCl₂(SMe₂)₂ in CH₂Cl₂ for 24 hours were irradiated.

Photochemical Quantum Yield Measurements

Freshly prepared potassium ferrioxalate was used as the standard actinometer ($\Phi_{s, 334 \text{ nm}} = 1.12$).²⁸ Photochemical quantum yields were determined according to Equation (1):

$$\Phi_{u} = \Phi_{s} \times (\Delta C_{u} \times V_{u} \times t_{s}) / (\Delta C_{s} \times V_{s} \times t_{u})$$
(1)

where Φ_s is the quantum yield of the standard; ΔC_s and ΔC_u are the changes in the concentrations of the standard actinometer and the unknown after irradiation at the λ_{max} of the unknown after t_s and t_u seconds, in solution volumes of V_s and V_u for the standard and the unknown, respectively. The standard and unknown solutions used

were concentrated enough to assume total absorption of the incident light, and UV-vis measurements were carried out after ten-fold dilutions to afford ΔC_s and ΔC_u .

Quantification of chlorobenzene by GC-MS

GC-MS measurements were carried out using a 1:150 split ratio for the injector, which was kept at 250 °C. The column temperature was initially kept at 40 °C for 5 minutes, then ramped up to 300 °C at a rate of 20 °C/min. Known solutions of chlorobenzene in CH_2Cl_2 (5.0, 10.0, 15.0, 20.0, and 25.0 mM) were analyzed using this method and their chlorobenzene peak integrations were used to establish a calibration curve. Finally, a photolyzed solution of **2**-Ph obtained by the procedure described above was analyzed and the concentration of chlorobenzene was determined from the calibration curve (Figure S9). The peak area for chlorobenzene in the photolyzed sample was 3.88×10^6 .

¹³C NMR detection of chlorobenzene

A solution of 2-Ph (9.7 mg, 0.01 mmol) in CH₂Cl₂ (0.5 mL) in the presence of 50 equivalents of SMe₂ was irradiated using a 100 W mercury arc lamp in a 5 mm NMR tube until the reaction was deemed to be complete as evidenced by ^{31}P NMR. 5.0 μL of acetonitrile was then injected in the tube as an additional internal standard. The tube was then sealed and the mixture was analyzed by ^{13}C NMR spectroscopy (Figure S7, maroon trace). Next, chlorobenzene (20.0 μL , 0.197 mmol) was injected into the tube and the resulting solution was again analyzed by ^{13}C NMR (Figure S7, light brown trace), resulting in a clear increase in the intensity of the chlorobenzene resonances.

ASSOCIATED CONTENT

Supporting Information

Additional experimental and computational details. Crystallographic data in cif format. Optimized structures in xyz format. These materials are available free of charge via the Internet at http://pubs.acs.org.

Accession Codes

CCDC 2101954 – 2101955 contain the supplementary crystallographic data for this paper. These data can be obtained free of charge via www.ccdc.cam.ac.uk/data_request/cif, or by emailing data_request@ccdc.cam.ac.uk, or by contacting The Cambridge Crystallographic Data Centre, 12 Union Road, Cambridge CB2 1EZ, UK; fax: +44 1223 336033.

AUTHOR INFORMATION

Corresponding Author

François P. Gabbaï – Department of Chemistry, Texas A&M University, College Station, Texas 77843, United States. orcid.org/0000-0003-4788-2998. Email: francois@tamu.edu

Authors

Mohammadjavad Karimi – Department of Chemistry, Texas A&M University, College Station, Texas 77843, United States.

Author Contributions

MK carried out the experimental work and co-wrote the manuscript with FPG. FPG oversaw the investigations.

Notes

The authors declare no competing financial interest.

Acknowledgments

This work is dedicated to Holger Braunschweig on the occasion of the 60th birthday. Financial support from the National Science Foundation (CHE-1856453), the Welch Foundation (A-1423), and Texas A&M University (Arthur E. Martell Chair of Chemistry) is gratefully acknowledged.

References

- 1. (a) Troian-Gautier, L.; Turlington, M. D.; Wehlin, S. A. M.; Maurer, A. B.; Brady, M. D.; Swords, W. B.; Meyer, G. J., Halide Photoredox Chemistry. *Chem. Rev.* **2019**, *119*, 4628-4683; (b) Yang, Z.; Zhang, J.; Kintner-Meyer, M. C. W.; Lu, X.; Choi, D.; Lemmon, J. P.; Liu, J., Electrochemical Energy Storage for Green Grid. *Chem. Rev.* **2011**, *111*, 3577-3613; (c) Nocera, D. G., Personalized Energy: The Home as a Solar Power Station and Solar Gas Station. *Chemsuschem* **2009**, *2*, 387-390.
- 2. (a) Hwang, S. J.; Powers, D. C.; Maher, A. G.; Anderson, B. L.; Hadt, R. G.; Zheng, S. L.; Chen, Y. S.; Nocera, D. G., Trap-Free Halogen Photoelimination from Mononuclear Ni(III) Complexes. *J. Am. Chem. Soc.* **2015**, *137*, 6472-5; (b) Perera, T. A.; Masjedi, M.; Sharp, P. R., Photoreduction of Pt(IV) Chloro Complexes: Substrate Chlorination by a Triplet Excited State. *Inorg. Chem.* **2014**, *53*, 7608–7621; (c) Teets, T. S.; Nocera, D. G., Halogen Photoreductive Elimination from Gold(III) Centers. *J. Am. Chem. Soc.* **2009**, *131*, 7411-7420.
- 3. (a) Lemon, C. M.; Hwang, S. J.; Maher, A. G.; Powers, D. C.; Nocera, D. G., Halogen Photoelimination from SbV Dihalide Corroles. *Inorg. Chem.* **2018**, *57*, 5333-5342; (b) Carrera, E. I.; McCormick, T. M.; Kapp, M. J.; Lough, A. J.; Seferos, D. S., Thermal and Photoreductive Elimination from the Tellurium Center of π -Conjugated Tellurophenes. *Inorg. Chem.* **2013**, *52*, 13779-13790.
- (a) Powers, D. C.; Hwang, S. J.; Anderson, B. L.; Yang, H.; Zheng, S. L.; Chen, Y. S.; Cook, T. R.; Gabbaï, F. P.; Nocera, D. G., Stereoelectronic Effects in Cl₂ Elimination from Binuclear Pt(III) Complexes. Inorg. Chem. 2016, 55, 11815-11820; (b) Powers, D. C.; Chambers, M. B.; Teets, T. S.; Elgrishi, N.; Anderson, B. L.; Nocera, D. G., Halogen photoelimination from dirhodium phosphazane complexes via chloride-bridged intermediates. Chem. Sci. 2013, 4, 2880-2885; (c) Cook, T. R.; McCarthy, B. D.; Lutterman, D. A.; Nocera, D. G., Halogen Oxidation and Halogen Photoelimination Chemistry of a Platinum-Rhodium Heterobimetallic Core. Inorg. Chem. 2012, 51, 5152-5163; (d) Teets, T. S.; Lutterman, D. A.; Nocera, D. G., Halogen Photoreductive Elimination from Metal-Metal Iridium(II)-Gold(II) Heterobimetallic Complexes. Inorg. Chem. 2010, 49, 3035-3043; (e) Cook, T. R.; Surendranath, Y.; Nocera, D. G., Chlorine Photoelimination from a Diplatinum Core: Circumventing the Back Reaction. J. Am. Chem. Soc. 2009, 131, 28-29; (f) Cook, T. R.; Esswein, A. J.; Nocera, D. G., Metal-Halide Bond Photoactivation from a Ptili-Auil Complex. J. Am. Chem. Soc. 2007, 129, 10094-10095; (g) Mann, K. R.; Lewis, N. S.; Miskowski, V. M.: Erwin, D. K.; Hammond, G. S.; Gray, H. B., Solar energy storage. Production of hydrogen by 546-nm irradiation of a dinuclear rhodium(I) complex in acidic aqueous solution. J. Am. Chem. Soc. **1977**, *99*, 5525-5526.
- 5. (a) Yang, H.; Gabbaï, F. P., Solution and Solid-State Photoreductive Elimination of Chlorine by Irradiation of a

- [PtSb]^{VII} Complex. *J. Am. Chem. Soc.* **2014**, *136*, 10866–10869; (b) Lin, T.-P.; Gabbaï, F. P., Two-Electron Redox Chemistry at the Dinuclear Core of a TePt Platform: Chlorine Photoreductive Elimination and Isolation of a TeVPt^I Complex. *J. Am. Chem. Soc.* **2012**, *134*, 12230-12238.
- 6. Sahu, S.; Gabbaï, F. P., Photoreductive Elimination of Chlorine from Antimony in an [SbPd]^{VII} Complex. *J. Am. Chem. Soc.* **2017**, *139*, 5035–5038.
- 7. Karimi, M.; Tabei, E. S.; Fayad, R.; Saber, M. R.; Danilov, E. O.; Jones, C.; Castellano, F. N.; Gabbaï, F. P., Photodriven Elimination of Chlorine From Germanium and Platinum in a Dinuclear Pt^{II}→Ge^{IV} Complex. *Angew. Chem. Int. Ed.* **2021**, *60*, 22352-22358.
- 8. (a) Kameo, H.; Ikeda, K.; Sakaki, S.; Takemoto, S.; Nakazawa, H.; Matsuzaka, H., Experimental and theoretical studies of Si-Cl and Ge-Cl σ -bond activation reactions by iridiumhydride. *Dalton Trans.* **2016**, *45*, 7570-7580; (b) Kameo, H.; Mushiake, A.; Isasa, T.; Matsuzaka, H.; Bourissou, D., Pd/Ni-Catalyzed Germa-Suzuki coupling via dual Ge–F bond activation. *Chem. Commun.* **2021**, *57*, 5004-5007.
- 9. (a) Takaya, J., Catalysis using transition metal complexes featuring main group metal and metalloid compounds as supporting ligands. *Chem. Sci.* **2021**, *12*, 1964-1981; (b) Takaya, J.; Miyama, K.; Zhu, C.; Iwasawa, N., Metallic reductant-free synthesis of α -substituted propionic acid derivatives through hydrocarboxylation of alkenes with a formate salt. *Chem. Commun.* **2017**, *53*, 3982-3985; (c) Zhu, C.; Takaya, J.; Iwasawa, N., Use of Formate Salts as a Hydride and a CO2 Source in PGeP-Palladium Complex-Catalyzed Hydrocarboxylation of Allenes. *Org. Lett.* **2015**, *17*, 1814-1817.
- 10. Álvarez-Rodríguez, L.; Brugos, J.; Cabeza, J. A.; García-Álvarez, P.; Pérez-Carreño, E., From a Diphosphanegermylene to Nickel, Palladium, and Platinum Complexes Containing Germyl PGeP Pincer Ligands. *Chem. Eur. J.* **2017**, *23*, 15107-15115.
- 11. Cabeza, J. A.; Fernández, I.; Fernández-Colinas, J. M.; García-Álvarez, P.; Laglera-Gándara, C. J., A Germylene Supported by Two 2-Pyrrolylphosphane Groups as Precursor to PGeP Pincer Square-Planar Group 10 Metal(II) and T-Shaped Gold(I) Complexes. *Chem. Eur. J.* **2019**, *25*, 12423-12430.
- 12. Herrmann, R.; Wittwer, P.; Braun, T., Platinum Complexes Bearing a Tripodal Germyl Ligand. *Eur. J. Inorg. Chem.* **2016**, *2016*, 4898-4905.
- 13. (a) Bauer, J.; Braunschweig, H.; Dewhurst, R. D., Metal-Only Lewis Pairs with Transition Metal Lewis Bases. *Chem. Rev.* **2012**, *112*, 4329-4346; (b) Hupp, F.; Ma, M.; Kroll, F.; Jimenez-Halla, J. O. C.; Dewhurst, R. D.; Radacki, K.; Stasch, A.; Jones, C.; Braunschweig, H., Platinum Complexes Containing Pyramidalized Germanium and Tin Dihalide Ligands Bound through σ, σ M·E Multiple Bonds. *Chem. Eur. J.* **2014**, *20*, 16888-16898.
- 14. (a) Galushko, A. S.; Prima, D. O.; Burykina, J. V.; Ananikov, V. P., Comparative study of aryl halides in Pd-mediated reactions: key factors beyond the oxidative addition step. *Inorganic Chemistry Frontiers* **2021**, *8*, 620-635; (b) Olsen, E. P. K.; Arrechea, P. L.; Buchwald, S. L., Mechanistic Insight Leads to a Ligand Which Facilitates the Palladium-Catalyzed Formation of 2-(Hetero)Arylaminooxazoles and 4-(Hetero)Arylaminothiazoles. *Angew. Chem. Int. Ed.* **2017**, *56*, 10569-10572; (c) Fors, B. P.; Watson, D. A.; Biscoe, M. R.; Buchwald, S. L., A Highly Active Catalyst for Pd-Catalyzed Amination Reactions: Cross-Coupling Reactions Using Aryl Mesylates and the Highly Selective Monoarylation of Primary Amines Using Aryl Chlorides. *J. Am. Chem. Soc.* **2008**, *130*, 13552-13554; (d) Grushin, V. V.; Alper, H., Transformations of Chloroarenes, Catalyzed by Transition-Metal Complexes. *Chem. Rev.* **1994**, *94*, 1047-1062.
- 15. Burford, N.; Frazee, C.; McDonald, R.; Ferguson, M.; Patrick, B.; Decken, A., Complexes of Stiboranium Mono-, Di-, and Tri-cations. *Chem. Eur. J.* **2018**, *24*, 4011-4013.
- 16. Ghidiu, M. J.; Pistner, A. J.; Yap, G. P. A.; Lutterman, D. A.; Rosenthal, J., Thermal versus Photochemical Reductive

- Elimination of Aryl Chlorides from NHC-Gold Complexes. *Organometallics* **2013**, *32*, 5026-5029.
- 17. For related alkyl-Cl bond forming processes, see: Blaya, M.; Bautista, D.; Gil-Rubio, J.; Vicente, J., Synthesis of Au(I) Trifluoromethyl Complexes. Oxidation to Au(III) and Reductive Elimination of Halotrifluoromethanes. *Organometallics* **2014**, *33*, 6358-6368.
- 18. Kang, K.; Liu, S.; Xu, C.; Lu, Z.; Liu, S.; Leng, X.; Lan, Y.; Shen, Q., C(sp2)–X (X = Cl, Br, and I) Reductive Eliminations from Well-Defined Gold(III) Complexes: Concerted or Dissociation Pathways? *Organometallics* **2021**, *40*, 2231-2239.
- 19. Winston, M. S.; Wolf, W. J.; Toste, F. D., Halide-Dependent Mechanisms of Reductive Elimination from Gold(III). *J. Am. Chem. Soc.* **2015**, *137*, 7921-7928.
- 20. Gygi, D.; Gonzalez, M. I.; Hwang, S. J.; Xia, K. T.; Qin, Y.; Johnson, E. J.; Gygi, F.; Chen, Y.-S.; Nocera, D. G., Capturing the Complete Reaction Profile of a C–H Bond Activation. *J. Am. Chem. Soc.* **2021**, *143*, 6060-6064.
- 21. Kameo, H.; Ikeda, K.; Bourissou, D.; Sakaki, S.; Takemoto, S.; Nakazawa, H.; Matsuzaka, H., Transition-Metal-Mediated Germanium–Fluorine Activation: Inverse Electron Flow in σ -Bond Metathesis. *Organometallics* **2016**, *35*, 713-719.
- 22. Zhao, X.-F.; Zhang, C., Iodobenzene dichloride as a stoichiometric oxidant for the conversion of alcohols into carbonyl compounds; two facile methods for its preparation. *Synthesis* **2007**, 551-557.
- 23. Sheldrick, G. M., SADABS, Version 2007/4, Bruker Analytical X-ray Systems, Inc., Madison, Wisconsin, USA. 2007.
- 24. Sheldrick, G. M., SHELXT integrated space-group and crystal-structure determination. *Acta Crystallographica Section A* **2015**, *71*, 3-8.
- 25. Sheldrick, G. M. *SHELXTL, Version 6.1*, Bruker Analytical X-ray Systems Inc.: Madison, Wisconsin, USA, 2000.
- Frisch, M. J.; Trucks, G. W.; Schlegel, H. B.; Scuseria, G. E.; Robb, M. A.; Cheeseman, J. R.; Scalmani, G.; Barone, V.; Petersson, G. A.; Nakatsuji, H.; Li, X.; Caricato, M.; Marenich, A. V.; Bloino, J.; Janesko, B. G.; Gomperts, R.; Mennucci, B.; Hratchian, H. P.; Ortiz, J. V.; Izmaylov, A. F.; Sonnenberg, J. L.; Williams; Ding, F.; Lipparini, F.; Egidi, F.; Goings, I.; Peng, B.; Petrone, A.; Henderson, T.; Ranasinghe, D.; Zakrzewski, V. G.; Gao, J.; Rega, N.; Zheng, G.; Liang, W.; Hada, M.; Ehara, M.; Toyota, K.; Fukuda, R.; Hasegawa, J.; Ishida, M.; Nakajima, T.; Honda, Y.; Kitao, O.; Nakai, H.; Vreven, T.; Throssell, K.; Montgomery Jr., J. A.; Peralta, J. E.; Ogliaro, F.; Bearpark, M. J.; Heyd, J. J.; Brothers, E. N.; Kudin, K. N.; Staroverov, V. N.; Keith, T. A.; Kobayashi, R.; Normand, J.; Raghavachari, K.; Rendell, A. P.; Burant, J. C.; Iyengar, S. S.; Tomasi, J.; Cossi, M.; Millam, J. M.; Klene, M.; Adamo, C.; Cammi, R.; Ochterski, J. W.; Martin, R. L.; Morokuma, K.; Farkas, O.; Foresman, J. B.; Fox, D. J. Gaussian 16 Rev. C.01, Wallingford, CT, 2016.
- 27. Glendening, E. D.; Landis, C. R.; Weinhold, F., NBO 6.0: Natural bond orbital analysis program. *J. Comput. Chem.* **2013**, *34*, 1429-1437.
- 28. (a) Kuhn, H. J.; Braslavsky, S. E.; Schmidt, R., Chemical actinometry (IUPAC technical report). *Pure Appl. Chem.* **2004**, *76*, 2105-2146; (b) Hatchard, C. G.; Parker, C. A., A New Sensitive Chemical Actinometer. II. Potassium Ferrioxalate as a Standard Chemical Actinometer. *Proc. R. Soc. London, Ser. A* **1956**, *235*, 518-536; (c) Parker, C. A., A New Sensitive Chemical Actinometer. I. Some Trials with Potassium Ferrioxalate. *Proc. R. Soc. London, Ser. A* **1953**, *220*, 104-116.

SYNOPSIS TOC: